

Linking Conditions for Models with Geometrical Basis

Rainer Burghardt

A-2061 Obritz 246, Obritz, Austria

Email: arg@aon.at

How to cite this paper: Burghardt, R. (2020) Linking Conditions for Models with Geometrical Basis. *Journal of Modern Physics*, 11, 355-364.

<https://doi.org/10.4236/jmp.2020.113022>

Received: February 11, 2020

Accepted: March 1, 2020

Published: March 4, 2020

Copyright © 2020 by author(s) and Scientific Research Publishing Inc.

This work is licensed under the Creative Commons Attribution International License (CC BY 4.0).

<http://creativecommons.org/licenses/by/4.0/>



Open Access

Abstract

Usually it is demanded that the metric and its 1st derivatives have to match at the boundary of two adjacent regions which are solutions to Einstein's field equation. We propose a new linking condition concerning gravitational models based on surfaces which could be embedded into a higher dimensional flat space. We probe this condition for the Schwarzschild interior and exterior solution.

Keywords

Linking Conditions, Short Discussions of Previous Papers, Schwarzschild Models, Flamm' Paraboloid

1. Introduction

The question of how spaces with different geometrical structures can be adapted to each other takes up a lot of space in gravity theory. Stellar objects are described by interior solutions of Einstein's field equations, their gravitational fields by exterior solutions. The two solutions have to be adjusted at the surface of the stellar object. The constituent quantities of the two geometries must merge smoothly into one another. Numerous authors have dealt with the problem of junction conditions in recent years.

O'Brien and Synge [1] examined boundary conditions and jump conditions on surfaces where quantities and their derivatives can be discontinuous. To be consistent, they required the metrics and their 1st and 2nd derivatives to match at the boundary of two regions. Cocke [2] considered a non-static infinite cylinder that he cut out of a Friedman universe. The cylinder was surrounded by a gravitational field. For the linking condition for both regions, he relied on the metric and its 1st derivatives, which he treated as the 1st and 2nd fundamental forms.

Israel [3] [4] basically relied on the 2nd fundamental forms of a 3-surface. He discussed the physical discontinuities and mismatching of coordinates. He was mainly concerned with expanding spherical shells and their linking condition to the surrounding empty space. Bonnor [5] and Faulkes found a class of interior solutions that match an exterior solution with a moving boundary. As a linking condition, they used the matching of the metric and its 1st derivatives. For the interior solution, they used the interior Schwarzschild solution in isotropic coordinates. Lanczos [6] [7] considered in connection with the de Sitter cosmos two-dimensional distributed singularities in which the metrics remain finite and constant but take a jump with respect to the normals. He interpreted this as a surface distribution of matter. In another paper, he delved into the problem in more detail and replied to a criticism from Sen. He dealt in detail with the question to what extent the 1st derivatives of the metric must coincide at the boundary of two regions. Abraham [8] examined the discontinuities using the Gauss and Codazzi equations and builds on the generalized expressions of the O'Brien-Synge relations. The problem of matching two regions is also significant in cosmology. Galaxies and clusters are thought to be embedded into an FRW universe with homogeneous mass distribution. At the boundaries of such vacuoles, linking conditions must be adhered. We cite the paper of Gilbert [9] as a representative of this topic. Leibowitz [10] investigates junction conditions in going over to admissible coordinates in the case of comoving coordinates. He claims that the Oppenheimer-Snyder solutions are correctly matched. Attempted modifications are shown to be incorrect. Lichnerowicz [11] investigated junction conditions which can match up to the 3rd derivative of the functions at the boundary. Sen [12] described the discontinuities on a surface that is covered with matter. The examination was carried out independent of coordinate systems. Taub [13] faced the existence of 3-dimensional hyper surfaces in spacetime across which there may be discontinuities in the stress-energy-momentum tensor and the metric and their derivatives. Kumar [14] examined spherical shells in an empty universe. The 1st derivatives of the metric are discontinuous at the boundaries. The stress-energy-momentum tensor is defined with δ -functions. Coburn [15] determined discontinuity relations for a charged incompressible fluid with conservation laws and the 1st law of thermodynamics, and using shock waves. Edelen [16] obtained a dynamical theory of discontinuity surfaces and the associated jump strengths of both physical and geometrical quantities. It forms the basis for a general analysis of galactic structures. Huber [17] considered adjacent regions with different structures. He deformed the metrics of these regions in such a way that the linking conditions are satisfied at the boundary surface of these two regions. McVittie [18] studied collapsing models in a more general way and tried linking conditions as well. Dautcourt [19] [20] dealt with the jumps of the stress-energy-momentum tensor and considered layers on surfaces moving with the velocity of light. Papapetrou [21] and Treder investigated discontinuities on hypersurfaces and the associated problem of shock waves.

Hayward [22] discussed regions with boundary surfaces at which the normal unit vector changes discontinuously. The validity of the second linking condition was surveyed by Nariai and Tomita [23] [24] [25] for the collapsing Oppenheimer-Snyder model [26]. Although the metric of the interior OS solution matches the exterior OS solution—the Schwarzschild solution in comoving coordinates—the 1st derivatives of the metrics do not match at the boundary. Nariai and Tomita found a new exterior solution for the OS model, which fulfills the second linking condition for the OS interior and is free of singularity. Mitra [27] found that the two Schwarzschild solutions do not comply with the 2nd linking condition. He proposed a new interior solution that meets both linking conditions at the boundary to the exterior solution.

Thus, the methods of the Nariai, Tomita, and Mitra to solve the linking problem were quite different. We want to go a third way and replace the condition that the 1st derivatives of the metrics have to match with another that is quite plausible and that connects the interior and exterior Schwarzschild solutions.

In Sec. 2, we present the Schwarzschild geometry in the light of Flamm's [28] original paper. We focus on the radii of curvature of the normal and inclined slices of the surfaces on which the Schwarzschild geometry is based. The metrics have the signature 4. The time-like arc element is defined by $dx^4 = i(c)dt$. The tag “ g ” indicates the value of a quantity at the boundary of the surfaces. In Sec. 3, we show that the 1st derivatives of the metrics of the Schwarzschild models do not match, and we replace them by the postulate that the surfaces representing the interior and exterior Schwarzschild solutions have to have common tangents at the boundary surface.

2. The Schwarzschild Geometry

The new linking condition which we have introduced has a limited area of application. It can only be applied to models that can be explained geometrically, *i.e.*, models which have an embedding. We require that

- I) the metrics match at the boundary.
- II) the tangents (cutting tangents) of the embedded surfaces coincide.

We inspect this procedure facing the interior and exterior Schwarzschild solutions. Both solutions can be embedded into a 5-dimensional flat space, whereby a 6th variable is necessary for the exterior solution. The space-like part of the interior solution is represented by a spherical cap, the exterior part by Flamm's paraboloid. The two regions have to be matched.

Using quasi-polar coordinates, the standard form of the exterior Schwarzschild metric is formed as follows:

$$ds^2 = \frac{1}{1 - \frac{2M}{r}} dr^2 + r^2 d\vartheta^2 + r^2 \sin^2 \vartheta d\varphi^2 - \left(1 - \frac{2M}{r}\right) dt^2. \quad (2.1)$$

Here r is the radial coordinate. The space-like part of the metric is the line element on Flamm's paraboloid. The parabolic intersection curve of this surface,

i.e., the Schwarzschild parabola is given by

$$R^2 = 8M(r - 2M). \tag{2.2}$$

R is the coordinate of the extra dimension in the 5-dimensional embedding space normal to r . Flamm has given a detailed geometrical explanation. His proposed geometrical properties are shown in **Figure 1**.

Differentiating (2.2) and substituting for R , we obtain the ascent of the Schwarzschild parabola

$$\frac{dR}{dr} = \frac{4M}{R} = \frac{\sqrt{\frac{2M}{r}}}{\sqrt{1 - \frac{2M}{r}}} = \tan \eta, \quad \sin \eta = \sqrt{\frac{2M}{r}}, \quad \cos \eta = \sqrt{1 - \frac{2M}{r}}, \tag{2.3}$$

with the angle η as the angle of ascent of the Schwarzschild parabola.

A straight line normal to Flamm’s paraboloid is cutting the coordinate R at the point P . The distance from P to the parabola is \mathcal{R} and the inclination η is the same as the angle of ascent of the parabola. From **Figure 1**, one can derive

$$r = \mathcal{R} \sin \eta. \tag{2.4}$$

The radius of curvature of the Schwarzschild parabola can be calculated using elementary methods and (2.4)

$$\rho = \sqrt{\frac{2r^3}{M}} = 2r \sqrt{\frac{r}{2M}} = \frac{2r}{\sin \eta} = 2\mathcal{R}.$$

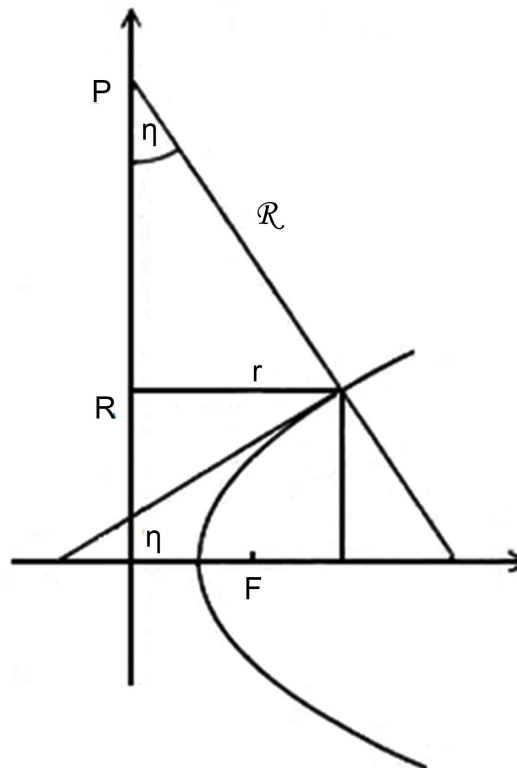


Figure 1. Flamm’s explanation of the parabolic properties.

Finally, we find the fundamental relations

$$\rho = 2\mathcal{R}, \quad \rho + \mathcal{R} = 3\mathcal{R}. \tag{2.5}$$

$3\mathcal{R}$ is the distance between the point P , the ‘‘pole’’ of the parabola and the base point of the curvature vector of the parabola, lying on the evolute of the Schwarzschild parabola, *i.e.*, on Neil’s parabola. With the insight of the factors 2 and 3, we have made a significant contribution to understand the interior Schwarzschild solution, as we will see later.

With the help of (2.3) the Schwarzschild metric can be written as

$$ds^2 = \frac{1}{\cos^2 \eta} dr^2 + r^2 d\mathcal{G}^2 + r^2 \sin^2 \mathcal{G} d\varphi^2 - \cos^2 \eta dt^2. \tag{2.6}$$

Further we put for the proper time

$$idT = \cos \eta idt = \rho \cos \eta di\psi. \tag{2.7}$$

Here, $i\psi$ is an imaginary angle and $\rho \cos \eta$ are the radii of a family of (open) pseudo circles (hyperbolae of constant curvature) lying in the $[x^{0'} = R, x^{4'}]$ -planes of the flat embedding space. $x^{4'}$ is an imaginary coordinate. A simple calculation shows that

$$\frac{1}{\cos \eta} dr = -\rho d\eta.$$

Thus, we are able to re-write the Schwarzschild line element as

$$ds^2 = \rho_i \rho_k d\eta^i d\eta^k, \quad i = k, \tag{2.8}$$

exhibiting all the curvatures of the slices of the surface described by the Schwarzschild metric. The curvature radii of the slices and the associated angles are

$$\begin{aligned} \rho_1 = \rho = \sqrt{\frac{2r^3}{M}}, \quad \rho_2 = r, \quad \rho_3 = r \sin \mathcal{G}, \quad \rho_4 = \rho \cos \eta \\ \eta^1 = \eta, \quad \eta^2 = \mathcal{G}, \quad \eta^3 = \varphi, \quad \eta^4 = i\psi. \end{aligned} \tag{2.9}$$

Tangents can be calculated on the intersection curves with these curvatures.

The line element of the interior Schwarzschild solution was given by Flamm as

$$ds^2 = \mathcal{R}^2 d\eta^2 + \mathcal{R}^2 \sin^2 \eta d\mathcal{G}^2 + \mathcal{R}^2 \sin^2 \eta \sin^2 \mathcal{G} d\varphi^2 - \frac{1}{4} [3\cos \eta_g - \cos \eta]^2 dt^2. \tag{2.10}$$

The space-like part of the metric is the metric of a hypersphere with the radius $\mathcal{R} = \text{const.}$ and the polar angle η . But only a part of that hypersphere is used.

A spherical cap with the aperture angle η_g is cut off from the hypersphere and placed on the Schwarzschild parabola from below. The intersection curves of the spherical cap and the Schwarzschild parabola at the boundary must have common tangents (cutting tangents). We will write about this later. Unfortunately, Flamm’s form of the interior metric is rarely found in literature. In the time-like part of the metric, the trigonometric functions are replaced by expressions with the radial variable r , by substituting $\sin \eta = r/\mathcal{R}$. This avoids to un-

derstand the geometry.

Differentiating $r = \mathcal{R} \sin \eta$, one finds

$$\mathcal{R}d\eta = \frac{1}{\cos \eta} dr .$$

Writing for the coordinate time using (2.5), one obtains

$$idt = \rho_g di\psi = 2\mathcal{R}di\psi , \tag{2.11}$$

where ρ_g is the curvature radius of the Schwarzschild parabola at the boundary surface. Finally, we have the equation for the metric of the interior Schwarzschild solution

$$ds^2 = \frac{1}{1 - \frac{r^2}{\mathcal{R}^2}} dr^2 + r^2 d\vartheta^2 + r^2 \sin^2 \vartheta d\varphi^2 + [3\mathcal{R} \cos \eta_g - \mathcal{R} \cos \eta]^2 di\psi^2 . \tag{2.12}$$

Here, we have met the magical factors 2 and 3 as explained in (2.5). The proper time of the interior Schwarzschild model is described by two concentric pseudo-circles with the radii $3\mathcal{R} \cos \eta_g$ and $\mathcal{R} \cos \eta$. This circle is lying in the $[x^0, x^4]$ -plane of the flat 5-dimensional embedding space¹.

We realize that the Schwarzschild interior solution is soldered to the exterior solution, because it contains elements of the exterior solution, *i.e.*, ρ_g the curvature radius of the Schwarzschild parabola at the boundary.

3. The Linking Conditions

We turn to the discussion of the linking conditions. Evidently, the 1st linking condition for the Schwarzschild solutions is satisfied. Their metrics coincide at the boundary. Considering the interior solution using (2.12) and putting $\eta = \eta_g$, one obtains

$$\frac{1}{\cos \eta_g} dr, \quad 2\mathcal{R} \cos \eta_g di\psi = \rho_g \cos \eta_g di\psi , \tag{3.1}$$

i.e., the corresponding expressions of the exterior metric (2.7) at the boundary surface.

It was Mitra [27], who showed that the 2nd linking condition cannot be applied to the Schwarzschild solutions. The first derivatives of the metrical coefficients do not match. The radial part of the line elements (2.6) and (2.12) for both solutions is

$$\frac{1}{\cos^2 \eta} dr^2 .$$

Differentiating the metrical factor, we get

$$g_{11|1} = \left(\frac{1}{\cos^2 \eta} \right)_{|1} = \frac{2 \sin \eta}{\cos^3 \eta} \eta_{|1} .$$

Here, all the indices are coordinate indices. Now one has to calculate $\eta_{|1}$ for both models. From

¹More details one can find in our monographs [29] [30].

$$\frac{1}{\cos \eta} dr = \mathcal{R} d\eta, \quad \frac{1}{\cos \eta} dr = -\rho d\eta$$

one has

$$\eta_{|1} = \frac{1}{\mathcal{R} \cos \eta}, \quad \eta_{|1} = -\frac{1}{\rho \cos \eta}.$$

Thus, recalling $\rho = 2\mathcal{R}$, one obtains the relations

$$g_{11|1} = \frac{2 \sin \eta}{\mathcal{R} \cos^4 \eta}, \quad g_{11|1} = -\frac{2 \sin \eta}{\rho \cos^4 \eta} = -\frac{\sin \eta}{\mathcal{R} \cos^4 \eta}. \quad (3.2)$$

Evidently, these relations are also valid at the boundary surface. However, they differ by the factor -2 , whereas the factor 2 is typically for the Schwarzschild geometry. Thus, the commonly accepted 2nd linking condition of O'Brien and Synge is not satisfied for the Schwarzschild geometry and has lost its legitimacy.

For the derivatives of the g_{44} one obtains for the interior solution

$$\begin{aligned} g_{44|1} &= \frac{1}{4} (3 \cos \eta_g - \cos \eta)^2_{|1} \\ &= \frac{1}{2} (3 \cos \eta_g - \cos \eta) \sin \eta \eta_{|1} \\ &= \frac{1}{2} (3 \cos \eta_g - \cos \eta) \sin \eta \frac{1}{\mathcal{R} \cos \eta} \end{aligned}$$

and at the boundary

$$g_{44|1} = \frac{1}{\mathcal{R}} \sin \eta_g.$$

For the exterior solution one has

$$g_{44|1} = (\cos^2 \eta)_{|1} = -2 \cos \eta \sin \eta \eta_{|1} = -2 \cos \eta \sin \eta \frac{1}{\rho \cos \eta} = -\frac{1}{\mathcal{R}} \sin \eta, \quad (3.3)$$

and at the boundary

$$g_{44|1} = -\frac{1}{\mathcal{R}} \sin \eta_g.$$

The difference in the signs can be explained with the fact that the curvature vectors \mathcal{R} and ρ have opposite directions. Robson [31] also recognizes that the 1st derivatives of the metric of the Schwarzschild models do not match at the boundary surface and he tries to force the match using a coordinate transformation. However, he drops this condition and agrees with the other authors to demand the coincidence of the 2nd fundamental forms.

In earlier papers we repeatedly mentioned that interior and exterior solutions should have common tangents at the boundary surface. We believed that this was a commonly accepted criterion for matching solutions. However, a careful study of the literature has shown that this requirement is not in use. In contrast, general validity is ascribed to the O'Brien-Synge method. Now we make up the proof that our requirement II provides functional results for the Schwarzschild geometry.

To calculate the tangents to the Flamm’s paraboloid, it is sufficient to face the equation of the Schwarzschild parabola (2.2). We already have calculated the ascent of the Schwarzschild parabola with (2.3), *i.e.*,

$$\frac{dR}{dr} = \tan \eta, \tag{3.4}$$

which is equally valid at the boundary surface.

For the interior solution we have to calculate the ascent of the circle

$$r^2 + R^2 = \mathfrak{R}^2, \quad R = \pm\sqrt{\mathfrak{R}^2 - r^2}, \quad \frac{dR}{dr} = \pm\frac{r}{R}.$$

with $r = \mathfrak{R} \sin \eta, R = \mathfrak{R} \cos \eta$ one finally obtains

$$\frac{dR}{dr} = \tan \eta.$$

Here, the sign is chosen to be “+” because the spherical cap is adapted to the Schwarzschild parabola from below. We recognize that the interior and the exterior surfaces have a common tangent (cutting tangent) at the boundary surface. But this is evident right from the beginning, because the curvature vectors \mathfrak{R} and ρ are lying in the same straight line at the boundary surface and are normal to the cap of the sphere and the Schwarzschild parabola and thus normal to the tangents of the two surfaces. Accordingly, the tangents have to coincide. We could have done without the calculation.

Lastly, we investigate the time-like parts of the models. Taking a glance at the interior metric (2.12), we find that the flow of time is characterized by two concentric pseudo circles with the radii $3\mathfrak{R} \cos \eta_g$ and $\mathfrak{R} \cos \eta$ founding a pseudo-ring sector. It is parameterized in the 5-dimensional flat space by

$$\begin{aligned} x^{0'} &= 3\mathfrak{R} \cos \eta_g \cos i\psi - \mathfrak{R} \cos \eta \cos i\psi \\ x^{4'} &= 3\mathfrak{R} \cos \eta_g \sin i\psi - \mathfrak{R} \cos \eta \sin i\psi \end{aligned}$$

Since both circles have the same ascents, it is sufficient to calculate the ascent of one circle, *i.e.*, for a specific slice $\eta = const.$

$$\begin{aligned} x^{0'2} + x^{4'2} &= \mathfrak{R}^2 \cos^2 \eta \\ \frac{dx^{0'}}{dx^{4'}} &= -\frac{x^{4'}}{x^{0'}} = -\tan i\psi, \quad \frac{dx^{0'}}{dt'} = -i \tan i\psi = th\psi. \end{aligned} \tag{3.5}$$

For the exterior solution, one has

$$\begin{aligned} x^{0'} &= \rho \cos \eta \cos i\psi \\ x^{4'} &= \rho \cos \eta \sin i\psi \end{aligned}$$

and the equation of the pseudo circle for a specific slice $\rho \cos \eta = const.$ is

$$\begin{aligned} x^{0'2} + x^{4'2} &= \rho^2 \cos^2 \eta \\ \frac{dx^{0'}}{dx^{4'}} &= -\frac{x^{4'}}{x^{0'}} = -\tan i\psi, \quad \frac{dx^{0'}}{dt'} = -i \tan i\psi = th\psi. \end{aligned} \tag{3.6}$$

The result is also valid at the boundary surface. Thus, one gets common tangents.

Once more we note that the last calculation is superfluous since the expressions for the radii of the two interior pseudo circles reduce for $\eta = \eta_g$ to

$$2\mathcal{R} \cos \eta_g = \rho_g \cos \eta_g .$$

The pseudo circles of the interior and exterior solutions coincide at the boundary surface and have the same tangents.

4. Conclusions

We showed that the interior Schwarzschild solution and the exterior Schwarzschild solution have common tangents at the boundary surface. We made this clear by calculating the ascents of the tangents of the two Schwarzschild solutions. Thus, the postulation that the tangents of surfaces representing gravitational models coincide at the boundary surface can serve as a linking condition and can replace the O'Brien-Synge condition, which does not apply to the Schwarzschild models.

Furthermore, it is quite likely that our method will also be applicable to the Reissner-Nordström model and to all models of the Kerr family.

Conflicts of Interest

The author declares no conflicts of interest regarding the publication of this paper.

References

- [1] O'Brien, S. and Synge, J.L. (1952) *Communications of the Dublin Institute for Advanced Studies*, No. 9, 1-20.
- [2] Cocke, W.J. (1966) *Journal of Mathematical Physics*, **7**, 1171-1178. <https://doi.org/10.1063/1.1705020>
- [3] Israel, W. (1966) *Nuovo Cimento*, **44**, 1-14. <https://doi.org/10.1007/BF02710419>
- [4] Israel, W. (1958) *Proceedings of the Royal Society of London. Series A*, **A248**, 404-414. <https://doi.org/10.1098/rspa.1958.0252>
- [5] Bonnor, W.B. and Faulkes, M.C. (1967) *Monthly Notices of the Royal Astronomical Society*, **137**, 239-251. <https://doi.org/10.1093/mnras/137.3.239>
- [6] Lanczos, K. (1922) *Annalen der Physik*, **24**, 539-543.
- [7] Lanczos, K. (1924) *Annalen der Physik*, **74**, 518-540. <https://doi.org/10.1002/andp.19243791403>
- [8] Abraham, R. (1962) *Journal of Mathematics and Mechanics*, **11**, 553-592. <https://www.jstor.org/stable/24900913> <https://doi.org/10.1512/iumj.1962.11.11033>
- [9] Gilbert, C. (1956) *Monthly Notices of the Royal Astronomical Society*, **116**, 678-683. <https://doi.org/10.1093/mnras/116.6.678>
- [10] Leibowitz, C. (1969) *Nuovo Cimento*, **60B**, 254-260. <https://doi.org/10.1007/BF02710226>
- [11] Lichnerowicz, A. (1971) *Comptes Rendus Chimie A*, **273**, 538.
- [12] Sen, N. (1924) *Annalen der Physik*, **73**, 365-396.

- <https://doi.org/10.1002/andp.19243780505>
- [13] Taub, A.H. (1957) *Journal of Mathematical Physics*, **10**, 370-388.
<https://doi.org/10.1215/ijm/1255380389>
- [14] Kumar, M.M. (1970) *Progress of Theoretical Physics*, **44**, 243-253.
<https://doi.org/10.1143/PTP.44.243>
- [15] Coburn, N. (1961) *Journal of Mathematics and Mechanics*, **10**, 361-391.
<https://www.jstor.org/stable/24900727>
<https://doi.org/10.1512/iumj.1961.10.10023>
- [16] Edelen, D.G.B. (1963) *Journal of Mathematical Analysis and Applications*, **2**, 247-263. <https://apps.dtic.mil/dtic/tr/fulltext/u2/407382.pdf>
[https://doi.org/10.1016/0022-247X\(63\)90050-7](https://doi.org/10.1016/0022-247X(63)90050-7)
- [17] Huber, A. (2019) Junction Conditions and Local Spacetimes in General Relativity.
- [18] McVittie, G.E. (1964) *The Astrophysical Journal*, **140**, 401-416.
<https://doi.org/10.1086/147937>
- [19] Dautcourt, G. (1964) *Mathematische Nachrichten*, **27**, 279-288.
<https://doi.org/10.1002/mana.19640270504>
- [20] Dautcourt, G. (1963) *Archive for Rational Mechanics and Analysis*, **13**, 55-58.
<https://doi.org/10.1007/BF01262683>
- [21] Papapetrou, A. and Treder, H.-J. (1961) *Mathematische Nachrichten*, **23**, 371-384.
<https://doi.org/10.1002/mana.1961.3210230605>
- [22] Hayward, G. (1993) *Physical Review D*, **47**, 3275-3280.
<https://doi.org/10.1103/PhysRevD.47.3275>
- [23] Nariai, H. and Tomita, K. (1966) *Progress of Theoretical Physics*, **35**, 777-785.
<https://doi.org/10.1143/PTP.35.777>
- [24] Nariai, H. and Tomita, K. (1965) *Progress of Theoretical Physics*, **34**, 155-172.
<https://doi.org/10.1143/PTP.34.155>
- [25] Nariai, H. (1965) *Theoretical Physics*, **34**, 173-186.
<https://doi.org/10.1143/PTP.34.173>
- [26] Oppenheimer, J.R. and Snyder, H. (1939) *Physical Review*, **56**, 455-459.
<https://doi.org/10.1103/PhysRev.56.455>
- [27] Mitra, A. (2010) No Uniform Density Star in General Relativity.
<https://arxiv.org/pdf/1012.4985.pdf>
<https://doi.org/10.1007/s10509-010-0567-8>
- [28] Flamm, L. (1916) *Physikalische Zeitschrift*, **17**, 448-454.
- [29] Burghardt, R. (2016) Spacetime Curvature. 1-597.
<http://members.wavenet.at/arg/EMono.htm>
- [30] Burghardt, R. (2016) Raumkrümmung. 1-623.
<http://members.wavenet.at/arg/Mono.htm>
- [31] Robson, E.H. (1972) *Annales Henri Poincaré*, **16**, 41-50.
<http://eudml.org/doc/75725>